Proceedings of the 4th ITB Graduate School Conference
Innovation and Discovery for Sustainability
July 6, 2023

2D Incompressible Flow Numerical Modeling of LSMPS Vortex Particle Method using Ellipsoidal Particle

Made Yogga Anggara Pangestu*, Pramudita Satria Palar & Lavi Rizki Zuhal

Faculty of Mechanical and Aerospace Engineering, Institut Teknologi Bandung, Jalan Ganesa 10, Bandung 40132, Indonesia
*Email: anggarapangestu@gmail.com

Abstract. Particle-based fluid simulation has been vastly developed in the recent age. In our groups, a vortex particle method (VPM) is developed using LSMPS method and Brinkman penalization. One of the issues in our program is to enhance performance since it still has a high computational cost. The particle distribution technique of ellipsoidal particles is a new method that intrigues this work. In this paper, the LSMPS–VPM fluid simulation program is being modified by ellipsoidal particle distribution. It was tested on a laminar boundary layer on a flat plate. The results have a significant computation cost reduction with computation time saved up to 53% and even more. The error increase is low and linearly proportional towards the elliptical ratio. By this result, it is very potential to implement this ellipsoidal particle technique on other fluid solvers in reducing the computational cost.

Keywords: *multiresolution; ellipsoidal particle; LSMPS; vortex particle method.*

1 Introduction

The Vortex Method is one of the methods used for incompressible flow numerical computation. It is a Lagrangian description based on vorticity properties. The growth of fluid motion is calculated from the velocity and vorticity. This method decouples the pressure leaving a simple governing equation of a Lagrangian diffusion of vorticity.

Vortex method simulation has matured since its development in the past two decades [1], which has the benefit of computing only the region in which the vorticity field is nonzero. This condition is very suitable for FSI simulation since the nonzero vorticity only occurred at the solid boundary and wake. In the current age, the vortex method has been vastly implemented in particle-based simulations, see the work by Rassmussen [7], Gazolla [8], and Dung [12].

A particle-based simulation is an old simulation scheme but is vastly being developed as of late. One of the particle-based methods is MPS introduced by Koshizuka [2], which is used to compute an incompressible fluid dynamic. This

method is improved by the least squared approach, namely Least Square MPS or LSMPS, which is also the work by Koshizuka et al. [10]. The particle-based simulation has the benefit of reducing the meshing time since generating particles is simpler than mesh. However, the particle-based simulation encounters a computational cost problem, each element evaluation must calculate the other elements globally. This caused a high computational time in the particle-based simulation. This kind of problem has been discussed for the rest of this age. Many methods have been developed to reduce the computational cost i.e., particle distributions and simulation algorithms. Particle distribution techniques, such as multiresolution distribution, are often implemented in many numerical simulations e.g., multiresolution LSMPS method by Tanaka [11]. A new particle distribution technique of ellipsoidal particles has been developed lately by Shibata [5] to reduce the cost of MPS simulation. This method is prevalently used for a problem case that is focused in one direction, such as in the work by Tanaka [4] of laser irradiation on a thin plate.

In this work, the ellipsoidal distribution method is implemented into the current existing VPM–LSMPS method by Pristiansyah [13]. The program modification will be tested on a boundary layer over a flat plate since this simulation has a direction focused on the normal plate direction. The ellipsoidal modified program is being compared to the original one in part of error and computational cost.

2 Theory

2.1 Vortex Particle Method

In the vortex particle method (VPM), vorticity ($\boldsymbol{\omega}$) becomes the calculation's basic property. Vorticity is related to the velocity by Eq.1.

$$\boldsymbol{\omega} = \nabla \times \boldsymbol{u} \tag{1}$$

The governing equation in VPM begins with the Navier – Stokes equations. For 2D incompressible flow, the governing equation of VPM is given in Eq. 2.

$$\frac{\partial \boldsymbol{\omega}}{\partial t} + \boldsymbol{u} \cdot \nabla \boldsymbol{\omega} = \nu \nabla^2 \boldsymbol{\omega} \tag{2}$$

The equation (Eq. 2) is solved by the splitting method [3], treating the Lagrangian motion and the diffusion as sequential calculation procedure in Eq. 3 and Eq. 4.

$$\frac{\partial \boldsymbol{x}}{\partial t} = \boldsymbol{u}(\boldsymbol{x}, t) \tag{3}$$

$$\frac{d\boldsymbol{\omega}}{dt} = \nu \nabla^2 \boldsymbol{\omega}(\boldsymbol{x}, t) \tag{4}$$

The equation Eq. 3 describes the Lagrangian motion of the particle while equation Eq. 4 describes the diffusion of the vorticity. The velocity itself is calculated using the relation of velocity curl (Eq.1). The velocity can be decomposed into the function of stream vector (Eq. 5). Then by using the relation of velocity curl and vector calculus identity, the stream function will be a Poisson equation toward the vorticity (Eq. 6).

$$\boldsymbol{u} = \nabla \times \boldsymbol{\psi} \tag{5}$$

$$\nabla^2 \boldsymbol{\psi} = -\boldsymbol{\omega} \tag{6}$$

By applying the green vortex relation, the Poisson equation (Eq. 6) will be transformed into Biot–Savart equation (Eq. 7).

$$\boldsymbol{u_\omega}(\boldsymbol{x}_i, t) = -\frac{1}{2\pi}\sum_{\boldsymbol{j=0}}^{\boldsymbol{N}} \frac{(\boldsymbol{x}_i - \boldsymbol{x}_j)}{|\boldsymbol{x}_i - \boldsymbol{x}_j|^2} \Gamma_j \times \hat{\boldsymbol{e}}_{\boldsymbol{z}} \tag{7}$$

$$\Gamma_j = \omega_{z,j} \delta V_j \tag{8}$$

Where $\hat{\boldsymbol{e}}_{\boldsymbol{z}}$ is the unit vector in z direction. In the Vortex Particle Method, the vorticity is discretized into the domain by particles carrying vorticity. Each particle has a vortex strength Γ discretized as in Eq. 8. The δV_j is the volume occupied by the particle, which might be considered as a volume of a cube.

A direct Biot-Savart calculation is high in cost, it is very common to be enhanced by a fast algorithm such as FMM or FTT. The FMM method is considered since it can solve even for random particle distribution [9]. This method is compatible with the multiresolution distribution in the LSMPS-VPM fluid solver. According to the Helmholtz decomposition, the absolute velocity must take the stream velocity into account (Eq. 9).

$$\boldsymbol{u}(\boldsymbol{x}, t) = \boldsymbol{u}_\infty(\boldsymbol{x}, t) + \boldsymbol{u_\omega}(\boldsymbol{x}, t) \tag{9}$$

2.2 Brinkman Penalization

The presence of the solid object as an obstacle in the domain needs additional treatment to the boundary region. Brinkmann Penalization is an immersed boundary condition method which is enforcing the boundary condition of the solid wall by adding a penalization term into the momentum equation (Eq. 10) [7].

$$\frac{\partial \boldsymbol{u}}{\partial t} = \lambda \chi (\boldsymbol{u_s} - \boldsymbol{u}) \tag{10}$$

The parameter λ is the penalization constant. The variable χ is a region mask which is a switch function between solid and fluid ($\chi = 0$ for fluid and $\chi = 1$ for solid). A smooth function called mollification kernel is applied to the variable χ

to provide smoothness, such that being able to calculate the spatial differential numerically. A good approach for this kernel is provided by Gazolla, et al [8] given in Eq. 11.

$$\chi = \begin{cases} 0 & r_n < -r_\epsilon \\ \frac{1}{2}\left(1 + \frac{r_n}{r_\epsilon} + \frac{1}{\pi}\sin\left(\pi\frac{r_n}{r_\epsilon}\right)\right) & -r_\epsilon \le r_n \le r_\epsilon \\ 1 & r_n > r_\epsilon \end{cases} \tag{11}$$

Where r_n is the normal distance from the nearest solid boundary in the inward direction and r_ϵ is half of the mollified region width. In the VPM, the velocity penalization is solved separately from the main governing equation. This equation may be solved explicitly or implicitly; however, a better implementation is the implicit one (Eq. 12) which shows a more stable simulation. The $\widetilde{\boldsymbol{u}}$ is the velocity after applying the penalization, while $\boldsymbol{u}$ and $\boldsymbol{u}_s$ is the particle and solid velocity respectively.

$$\widetilde{\boldsymbol{u}} = \frac{\boldsymbol{u} + \lambda\chi\Delta t\, \boldsymbol{u}_s}{1 + \lambda\chi\Delta t} \tag{12}$$

The penalized velocity is used to update the vorticity given in Eq.13,14, and 15 .

$$\Delta\widetilde{\boldsymbol{u}} = \widetilde{\boldsymbol{u}} - \boldsymbol{u} \tag{13}$$

$$\Delta\widetilde{\boldsymbol{\omega}} = \nabla \times \Delta\widetilde{\boldsymbol{u}} \tag{14}$$

$$\widetilde{\omega} = \omega + \Delta\widetilde{\omega} \tag{15}$$

2.3 Least Square Moving Particle Semi-Implicit

The Least Square Moving Particle Semi-Implicit (LSMPS) method is a mesh-free Lagrangian approach for numerical analysis of incompressible flow that was developed by Koshizuka and Tamai [10]. This method provides a spatial differential operator for particle-based discretization. LSMPS shows high stability and accuracy for its operator, even in random particle distribution. LSMPS has two main types of spatial differential operators: LSMPS type A and LSMPS type B, both to calculate the spatial differential on the particle and at any arbitrary position respectively. The LSMPS spatial operator is given in Eq. 16.

$$\boldsymbol{D_x f^h}(\boldsymbol{x}) = \boldsymbol{H}_{r_s}\boldsymbol{M}_i^{-1}\boldsymbol{b}_i \tag{16}$$

In which the spatial differential of function $f(\boldsymbol{x})$ is a function of the matrix $\boldsymbol{H}_{r_s}$, moment matrix $\boldsymbol{M}_i$, and moment vector $\boldsymbol{b}_i$. Each of these matrices and the notation is given in Eq. 17, 18, 19, and 20.

$$\boldsymbol{D}_{\boldsymbol{x}} \coloneqq \left\{\frac{\partial^{|\boldsymbol{\alpha}|}}{\partial \boldsymbol{x}^{\boldsymbol{\alpha}}} \mid 1 \leq |\boldsymbol{\alpha}| \leq p\right\} \tag{17}$$

$$\boldsymbol{H}_{r_s} \coloneqq \mathrm{diag}\left\{\left\{r_s^{-|a|} a!\right\}_{1\leq|a|\leq p}\right\} \tag{18}$$

$$\boldsymbol{M}_i \coloneqq \sum_{j\in\Lambda_i}\left(\boldsymbol{w}\left(\|\boldsymbol{x_j}-\boldsymbol{x_i}\|\right)\boldsymbol{p}\left(\frac{\|\boldsymbol{x_j}-\boldsymbol{x_i}\|}{r_s}\right)\boldsymbol{p}^{\boldsymbol{T}}\left(\frac{\|\boldsymbol{x_j}-\boldsymbol{x_i}\|}{r_s}\right)\right) \tag{19}$$

$$\boldsymbol{b}_i \coloneqq \sum_{j\in\Lambda_i}\left(\boldsymbol{w}\left(\|\boldsymbol{x_j}-\boldsymbol{x_i}\|\right)\boldsymbol{p}\left(\frac{\|\boldsymbol{x_j}-\boldsymbol{x_i}\|}{r_s}\right)\left(\boldsymbol{f}(\boldsymbol{x_j})-\boldsymbol{f}(\boldsymbol{x_i})\right)\right) \tag{20}$$

A new operator notation is used for compacity, the definition can be found in the original paper [10]. The variable p is the highest order of the spatial differential to be calculated. There is a weight function $\boldsymbol{w}$ is given by as the quadratic weight function (Eq. 21).

$$\boldsymbol{w}(\boldsymbol{x}, r_e) = \begin{cases}\left(1-\frac{\|x\|}{r_e}\right)^2 & ,0 \leq \|x\| \leq r_e \\ 0 & ,\|x\| > r_e\end{cases} \tag{21}$$

Where r_e is an effective radius of the neighbour evaluation. The function $\boldsymbol{p}(x)$ is a vector given in Eq. 22.

$$\boldsymbol{p}(\boldsymbol{x}) \coloneqq \{\boldsymbol{x}^{\boldsymbol{\alpha}} \mid 1 \leq |\boldsymbol{\alpha}| \leq p\} \tag{22}$$

For a complete description and derivation, see the original paper by Tamai and Koshizuka [10].

2.4 Ellipsoidal Particle Modification

Ellipsoidal (or Elliptical in 2D) particle is a particle distribution technique that allows the particle resolution variates in a specific direction. This model is first introduced by Shibata et al [5] in reducing the computational cost of MPS simulation. It has been implemented on an energy study by Tanaka et al [4] in computing laser irradiation on a thin plate. In the elliptical particle, each direction is characterized by an elliptical ratio of $E = \{E_i \mid 1 \leq i \leq \dim\}$ that is the extension factor from circular particle size. For a simulation that has a high property gradient in a specific direction such as laser irradiation in a thin plate [4], the resolution can be set finer only at this direction by using the elliptical particle model, so that the increase of particle number is lower than just set a finer resolution in the circular form.

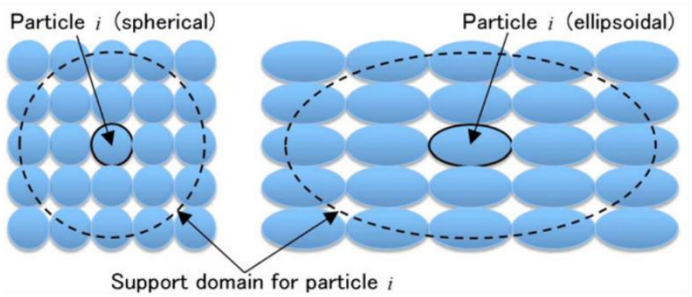

Figure 1 The support domain schematic between circular and elliptical particles.

In the elliptical particle scheme, the influence region (or support domain) must be elliptical, as shown in **Figure 1**. In order to apply the standard LSMPS operator in elliptical particle, the particle distribution need to be transformed into a circular distribution. The transformed position ($\boldsymbol{x}^*$) are calculated by the relation Eq. 23.

$$\boldsymbol{x}^* = \left\{ \frac{x_i}{E_i} \mid 1 \leq i \leq \dim \right\} \tag{23}$$

The LSMPS spatial difference is then performed as it should be in the transformed circular coordinate. The differential result from Eq. 17 then must be transformed back into its initial distribution (*elliptical*) by using Eq. 24.

$$\boldsymbol{D}_{\boldsymbol{x}^*} = \boldsymbol{\Lambda} \boldsymbol{D}_{\boldsymbol{x}} \tag{24}$$

where $\boldsymbol{D}_{\boldsymbol{x}^*}$ and $\boldsymbol{D}_{\boldsymbol{x}}$ is an array (may be treated as a vector) of differential in transformed circular distribution and initial elliptical distribution respectively and the matrix $\boldsymbol{\Lambda}$ is defined in Eq. 25.

$$\boldsymbol{\Lambda} := \mathrm{diag}\{E^{\boldsymbol{\alpha}} \mid 1 \leq |\alpha| \leq p\} \tag{25}$$

In the vortex particle method, the occupied volume (Eq. 8) will have a factor of the elliptical ratio. The volume will calculated using Eq. 26.

$$\delta V_i^* = \delta V_i \prod_{i=1}^{\dim} E_i \tag{26}$$

2.5 Numerical Simulation Procedure

The numerical computation of the VPM–LSMPS program solver is given by the following procedure:

1. ***Domain initialization***, particles are distributed into the domain using the given input parameter.
2. ***Neighbor particle evaluation***, each particle is evaluated to obtain the ID list of neighboring particles.

3. ***Solver Iteration***, calculate the simulation at each time step by the following sequence.
   a. ***Vorticity penalization***, using Brinkmann penalization to penalize velocity then update the vorticity. Use Eq. 16 to calculate the curl of velocity.
   b. ***Velocity calculation***, using FMM acceleration algorithm to compute the velocity Biot-Savart.
   c. ***Splitting method***, compute the governing equation on the domain using the splitting method algorithm. Use Eq. 16 to calculate the diffusion of vorticity.
   d. ***Particle redistribution***, redistributes the particle position into a regular distribution using LSMPS B interpolation of Eq. 16.
   e. Save particle state data.

3 Problem Description

In implementing the elliptical particle model to the LSMPS-VPM the main operator of LSMPS must be tested under the elliptical modified schemes. The LSMPS solver is being tested using a testing function. The implementation of the elliptical modified schemes in the LSMPS-VPM solver then is tested on a boundary layer flow problem.

3.1 LSMPS Elliptical Particle Modification Test Case

A function similar to the vorticity field of the boundary layer over the flat plate is chosen as the test function. As the vorticity is related to a decaying function, a bell curve-like function is adapted with some modification for the test function (see Eq. 27).

$$f(x,y) = \exp\left(-\frac{y^2}{x}\right) \tag{27}$$

Because the test function has a singularity at $x = 0$, the domain of simulation will exclude $x = 0$, taking only a squared domain bounded by $x = [1, 11]$ and $y = [0, 10]$. The LSMPS operator is used to calculate the first x derivative ($\partial f/\partial x$), first y derivative ($\partial f/\partial y$), and Laplacian ($\nabla^2 f$) of the test function. There are 3 elliptical ratio variations in the x direction only of $E_x = \{2,5,10\}$ also a circular particle (explicitly $E_x = 1$). The calculation schematic between the elliptical modification and the original LSMPS method is also compared to observe the effectiveness of the elliptical modification.

3.2 VPM-LSMPS Test Case: Boundary Layer Simulation

The ellipsoidal particle modification of the VPM-LSMPS program is tested using the flow case of a laminar boundary layer over a flat plate. The boundary layer over a semi-infinite flat plate has an analytical solution of Blasius. By the limitation of computational cost, the flat plate is set to have a finite length but long enough to be able to compare to the Blasius solution. An equivalent ANSYS fluent simulation is also performed for benchmark comparison.

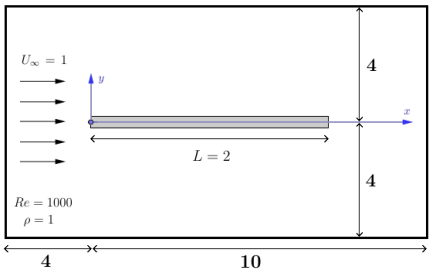

Figure 2 Flat plate simulation configuration.

The simulation parameter is given by the following data:

- Reynolds number of $\mathrm{Re} = 1000$
- Stream velocity of $U_\infty = 1$ m/s
- Density of $\rho = 1$ kg/m^3
- Plate length $L = 2$ m
- Plate thickness of $t = 0.02$ m

The domain size is 8×14 m considering the portion of the downstream, this configuration is depicted in **Figure 2**. The elliptical particle are tested up until $E_x = 10$. There are 5 elliptical ratio variations of $E_x = \{1.5, 3, 5, 7.5, 10\}$. The boundary layer property profile of each variation will be evaluated at half plate length $x = 0.5L$.

4 Data Result and Analysis

4.1 LSMPS Testing on Ellipsoidal Particle Distribution

The analytical solution of the test function differential and the function itself has a contour plot shown in **Figure 3**. For the sake of visualization, the domain is displayed between $x = [1, 8]$ and $y = [0, 4]$. The laplacian calculation using LSMPS-A in an elliptical modified LSMPS scheme of each elliptical ratio variation is shown in **Figure 4**.

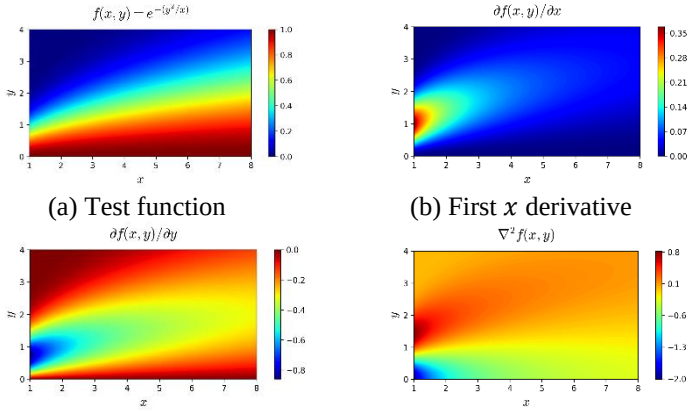

(a) Test function (b) First x derivative

(c) First y derivative (d) Laplacian

Figure 3 Contour plot of the test function (analytical solution)

The result of each differential calculation is compared to the analytical solution using a global error evaluation L_2 norm error. The calculation schematic of the original LSMPS is being compared with the elliptical modified one. The original one is named as ***regular scheme*** while the elliptical modified is named as ***elliptical scheme***. The global error summary for each differential calculation result is provided in **Table 1**.

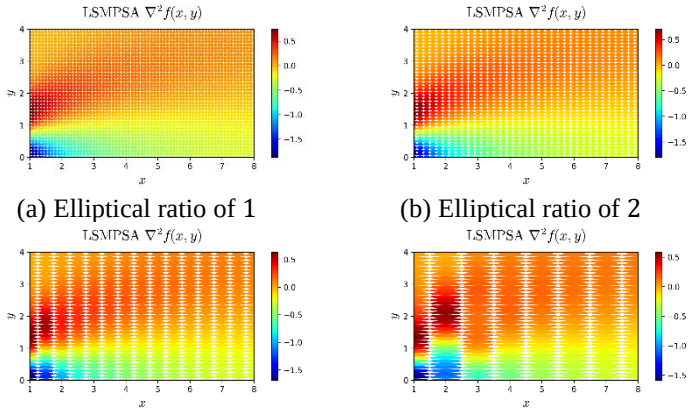

(a) Elliptical ratio of 1 (b) Elliptical ratio of 2

(c) Elliptical ratio of 5 (d) Elliptical ratio of 10

Figure 4 The LSMPS-A calculation result of Laplacian of each e_x variation

A better representation of the error data is given by an error plot (see **Figure 5**). In the error plot, the L_2 norm error of each elliptical ratio variation is normalized by the L_2 norm error of the circular distribution ($E_x = 1$). The first observation shows that, without using the elliptical modification schematic, the error is significantly larger. Since in the elliptical modified scheme a proper support region is used for the LSMPS calculation, this scheme calculates more accurately than the ***regular scheme***. The second observation is the linearity between the normalized error with the elliptical ratio. As shown in **Figure 5**, the ***elliptical schemes*** have a linear trend for each differential calculation.

Table 1 The L_2 norm error summary data.

Numerical Scheme	***Elliptical Ratio*** (E_x)	***Particle Number***	***L_2 Norm error*** ($\times 10^{-2}$)		
			$\partial f/\partial x$	$\partial f/\partial y$	$\nabla^2 f$
Elliptical Scheme	1	10201	0.95	0.6	1.97
	2	5050	1.54	0.65	3.9
	5	2020	6.17	1.7	10.62
	10	1010	16.3	4.52	26.97
Regular Scheme	1	10201	0.95	0.6	1.97
	2	5050	50.93	2.48	13.22
	5	2020	82.34	12.39	50.36
	10	1010	92.76	30.6	93.39

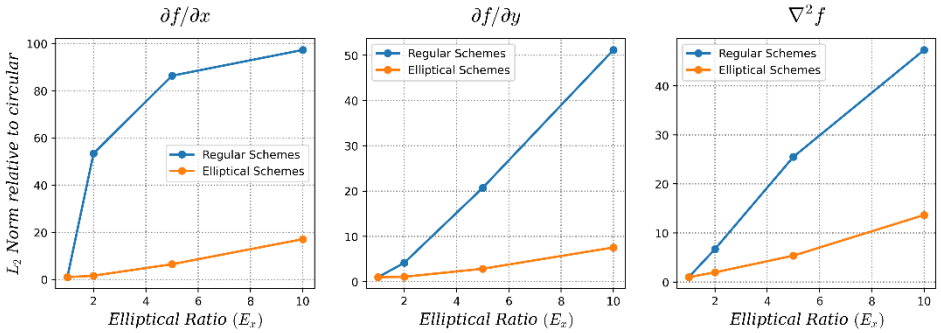

Figure 5 The L_2 Norm error relative to the circular distribution (note that the relative L_2 norm error of circular distribution $E_x = 1$ is equal to 1).

4.2 Boundary Layer Simulation of Ellipsoidal Particle

The flow parallel to an impulsively started flat plate is considered a benchmark flow problem. The particle size in the boundary layer simulation is small enough to get the boundary layer detail. The size corresponds to $y/\delta = 0.09$ at $x = 0.5L$ are used which results in particle core diameter of $\sigma = 0.004$. A prior test using coarse particle size results in the steady-state occurred after 6 units of time. To

perform a confident result, the simulation time is set longer with the value of 15 units of time, while the time step is set to be $\Delta t = 0.004$.

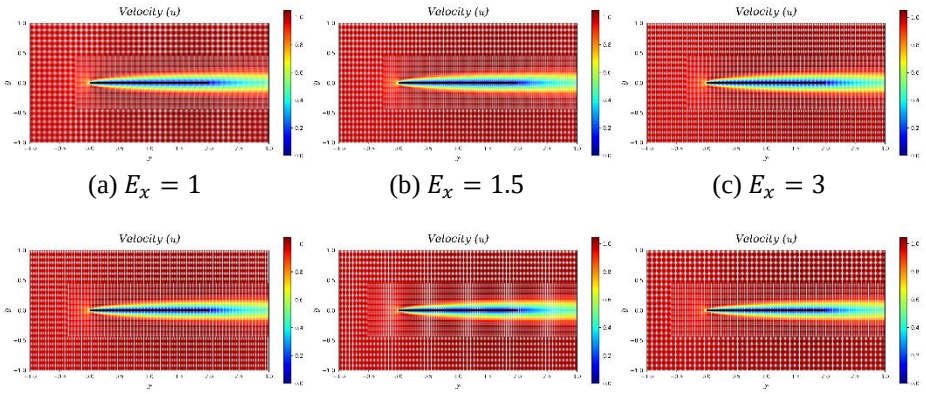

(a) $E_x = 1$ (b) $E_x = 1.5$ (c) $E_x = 3$

(d) $E_x = 5$ (e) $E_x = 7.5$ (c) $E_x = 10$

Figure 6 Velocity profile of each elliptical ratio variation at steady state

The result of the boundary layer velocity contour plot of each elliptical ratio is given in **Figure 6**. The numerical result of each elliptical particle distribution shows a similar contour toward the circular distribution. By visual observation, the elliptical modification of VPM–LSMPS is capable of simulating elliptical particle distribution very well. A detailed observation is performed by taking the velocity and vorticity profiles in the normal plate direction (y direction) at the half plate ($x = 0.5L$). Each of the elliptical ratio variations is compared to the Blasius as initial confirmation. A simulation result by a commercial solver of Fluent ANSYS in a similar configuration is also conducted for the benchmark data. This profile data is displayed in **Figure 7**. Each variation is plotted in the nondimensional form of $\eta(y) = y\sqrt{\frac{U_\infty}{\nu x}}$, $\hat{u}(u) = \frac{u}{U_\infty}$, and $\hat{\omega}(\omega_z) = \omega_z\sqrt{\frac{\nu x}{{U_\infty}^3}}$ where $x = 0.5L$ and $\nu = \frac{U_\infty L}{Re}$.

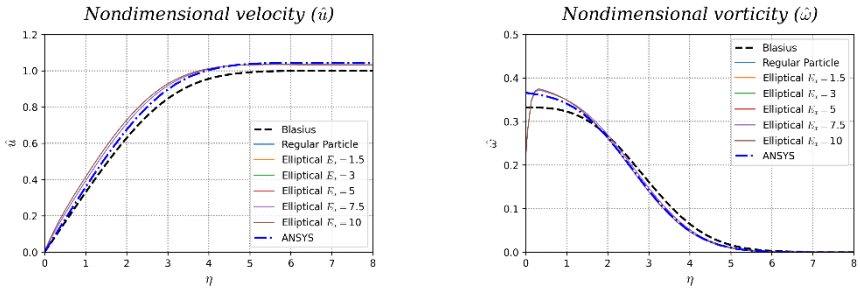

(a) (b)

Figure 7 The (a) velocity profile and (b) vorticity profile of each numerical simulation overlayed with benchmark solution in non-dimensional form.

The simulation result of each variation has a deviation toward the Blasius solution because the Blasius condition of no pressure gradient and the long plate is not fulfilled in the simulation. The comparison to the ANSYS simulation result shows a very close curve. However, at the region near the wall, the boundary layer profile of each elliptical variation shows a slight deviation toward the ANSYS solution, especially the vorticity profile shows a rising curve right after the wall ($\eta = 0$). This condition is caused by the mollification region effect of the Brinkman Penalization. A better no-slip boundary condition enforcement is needed for more accurate near-wall calculation, yet the Brinkman Penalization still provide a good calculation away from the wall. Compared to the circular particle distribution (named with regular particles), each of the elliptical variations shows a very close curve.

Table 2 The L_2 norm relative difference of velocity and vorticity profile of each elliptical ratio toward the regular particle

Variation	Elliptical Ratio (E_x)	L_2 norm ($\times 10^{-2}$)	
		Velocity ($\hat{u}$)	Vorticity ($\hat{\omega}$)
Elliptical 1	1.5	0.17	0.31
Elliptical 2	3	0.31	0.53
Elliptical 3	5	0.66	1.41
Elliptical 4	7.5	1.60	2.98
Elliptical 5	10	2.91	5.26

Error quantification of the elliptical particle toward the circular particle is represented by L_2 norm error, provided in **Table 2**. It is clear, as the elliptical ratio gets large the L_2 norm increases. At small elliptical ratio (up until $E_x = 3$) the L_2 norm is relatively small. While at a larger elliptical ratio, the relative error is increasing larger.

Table 3 Elliptical variation of flow over flat plate simulation summary data

Variation	Elliptical Ratio (E_x)	Particle Number	Computational Time Each Iteration (s)	Total Computational Time (s)
Regular	1	1823710	167.31	627026
Elliptical 1	1.5	1218653	79.05	296169
Elliptical 2	3	612427	24.5	91243
Elliptical 3	5	369830	13.01	44117
Elliptical 4	7.5	248957	7.17	26882
Elliptical 5	10	188095	5.43	20344

The computational cost of the simulation is provided in **Table 3**. At $E_x = 1.5$ the particle number is cut by 33% with computational time saved by 53%. It is reduced even more at $E_x = 10$ the particle number is cut by 90% with computational time saved by 97%. The computational time plot with elliptical ratio also the error to saving time trade-off plot is provided in **Figure 8**. The saving time is the cut of computational time toward the circular particle distribution computational time, while the error using the velocity L_2 norm error. The **Figure 8.a** shows the computational time has an exponential decaying trend by the elliptical ratio. From the chart in **Figure 8.b**, the error is significantly increased to achieve a higher computational saving time above 80%. For saving time below 80%, the error is still low below 3×10^{-3}. This error increase is considered low compared to the time-saving. For practical use, better to use an elliptical ratio at the trend bending point (on this flat plate test is $E_x = 3$, see **Figure 8.b**).

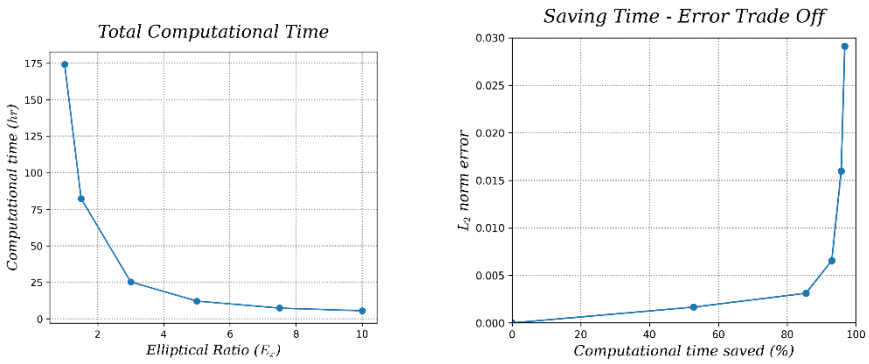

(a) (b)

Figure 8 The plot of (a) computational time by elliptical ratio variation and (b) the L_2 norm error of velocity toward the saving time

5 Conclusion

This work shows a significant cost decrease by implementing the ellipsoidal particle and still preserving the level of accuracy pretty well. In this work, the elliptical particle modification is successfully implemented on the VPM–LSMPS program solver and is capable of resulting in a good simulation. This modification program is applied on flow over a flat plate to observe the boundary layer as a flow case with one direction focus which is the advantage of using the elliptical particle distribution. The elliptical modification of the LSMPS method is first confirmed using a boundary layer-like function. An error observation using L_2 norm show a linear trend of global error toward the elliptical ratio. The VPM–LSMPS program modification simulation on the flow over a flat plate shows an exponential decrease in computational time. The boundary layer profile result of each elliptical ratio variation is compared with Fluent ANSYS simulation, showing a close profile between each. An error comparison using L_2 norm to the velocity and vorticity profile shows a relatively small error increase for the elliptical ratio below $E_x = 3$, while becoming large for a higher elliptical ratio.

This work shows the benefit of implementing ellipsoidal particle modification in a scientific simulation, especially one which is having a main focus on one direction. The usage of the ellipsoidal particle will reduce the computational cost by a significant amount of 53% with only an elliptical ratio of 1.5 while preserving the accuracy level.

Acknowledgement

This work is fully supported by the Flow Science and Engineering Lab in the Faculty of Mechanical and Aerospace Engineering.

References

[1] Cottet, G.-H., Koumoutsakos, P. D. et al., *Vortex methods: Theory and practice*, vol. 8, Cambridge university press Cambridge, 2000.

[2] Koshizuka, S., *Moving particle semi-implicit method*. Matthew Deans, Elsevier, 2018.

[3] Chorin, A., *Numerical study of slightly viscous flow*, Journal of Fluid Mechanics, 57, pp. 785–796, 1973.

[4] Tanaka, M., Cardoso, R., & Bahai, H., *Modification of the lsmps method for the conservation of the thermal energy in laser irradiation processes*, International Journal for Numerical Methods in Engineering, 117 (2), pp. 161–187, 2019.

[5] Shibata, K., Koshizuka, S., Masaie, I., *Cost reduction of particle simulations by an ellipsoidal particle model*, Computer Methods in Applied Mechanics and Engineering, 307, pp. 411-450, 2016.
[6] Angot, P., Bruneau, C.-H., & Fabrie, P., *A penalization method to take into account obstacles in incompressible viscous flows*, Numerische Mathematik, 81, pp. 497–520, 1999.
[7] Rasmussen, J. T., *Particle methods in bluff body aerodynamics*, Doctoral dissertation, Technical University of Denmark, 2011.
[8] Gazzola, M., Chatelain, P., Van Rees, W. M., & Koumoutsakos, P., *Simulations of single and multiple swimmers with non-divergence free deforming geometries*, Journal of Computational Physics, 230 (19), pp. 7093–7114. 2011.
[9] Greengard, L., & Rokhlin, V., *A new version of the fast multipole method for the laplace equation in three dimensions*, Acta numerica, 6, pp. 229–269, 1997.
[10] Koshizuka, S., & Tamai, T., *Least squares moving particle semi-implicit method*, Computational Particle Mechanics (CPM), 1, pp. 1–18, 2014.
[11] Tanaka, M., Cardoso, R., & Bahai, H., *Multi-resolution MPS method*, Journal of Computational Physics, 359, pp. 106–136, 2018.
[12] Dung, D. V. *Lagrangian vortex method with brinkman penalization*, Doctoral dissertation, Institut Teknologi Bandung, Bandung, 2015.
[13] Pristiansyah, A., *Improvement of vortex particle method using multi–resolution least square moving particle semi-implicit (LSMPS) method*, Master's thesis, Institut Teknologi Bandung, Bandung, 2019.